

Protein-Nucleic Acid Interactions. II. Oligopeptide-Polyribonucleotide Binding Studies*

Samuel A. Latt† and Herbert A. Sober

ABSTRACT: Equilibrium dialysis measurements were made at pH 7 and 4° over a range of NaCl concentrations of the binding of individual oligomers of the (L-lysine)_n- ϵ -N-DNP-L-lysine series ($n = 3, 4, 5, 6, 7$, or 8) to synthetic polynucleotides, principally poly (I + C) and poly (A + U). Evidence is presented for a 1:1 lysine:phosphorus ratio in the soluble complexes formed. Binding was stronger to poly (I + C) than to poly (A + U). Both the total binding energy and the

difference between the binding energies to poly (I + C) and poly (A + U) increased linearly with oligolysine chain length.

The strong inhibition of the binding by NaCl is interpreted in terms of a competition between Na⁺ and the oligolysines for the polynucleotide phosphates. A general theory of reversible colinear oligomer-polymer interactions is presented and used to extract parameters from the binding data.

Previous work from this laboratory examining the resistance of polylysine-RNA complexes to nonspecific nucleases has suggested the existence of base composition specificity in the polylysine-RNA interaction (Sober *et al.*, 1966). However, the experiments measured only the end result of a chain of events which included polylysine-RNA complex formation, nuclease digestion of uncomplexed RNA, and precipitation of the residual complex with a lysine:nucleotide ratio of 1. The observed protection specificity could have resulted from any of these steps.

The present study represents an attempt to gain some understanding of the polylysine-RNA complex formation from equilibrium dialysis measurements of the binding of members of a labeled oligolysine series (ϵ -DNP-Lys(Lys)_n ($n = 3-8$)) to synthetic polyribonucleotides (principally poly (I + C) and poly (A + U)).¹ The information sought includes the strength of the oligolysine-polynucleotide interaction, its stoichiometry, and its specificity or selectivity. Use of chromatographically purified oligolysines of known chain length, each oligomer labeled with a single dinitrophenyl (DNP) group on the ϵ -NH₂ of the C-terminal lysine, serves to increase the sensitivity of detection of specificity and permits the quantitative analysis of experimental binding curves in terms of a

model of reversible colinear adsorption of the oligomer to the polymer.

Materials

Chemicals. Inorganic chemicals were reagent grade. Cacodylic acid was purchased from K & K Laboratories. Deionized distilled water was used for all buffers. CHCl₃ and sodium azide (a few milligrams per liter) were added to buffers to retard growth of microorganisms. Glassware washed in chromic acid was subsequently rinsed in nitric acid-sulfuric acid to remove chromate. Nalgene containers were used in preference to glass to which polylysine is known to adsorb (Nevo *et al.*, 1955).

Oligolysines. A crude mixture of ϵ -DNP-Lys(Lys)_n ($\bar{n} = 13$) was obtained from the Weizmann Institute of Science, Rehovoth, Israel, under Collaborative Research Agreement No. 235103 with the National Institutes of Health. The polymers had been initiated by the benzyl ester of ϵ -N-DNP-L-lysine added to a solution of the N-carboxy- α -anhydride of benzyloxycarbonyl-L-lysine. Following polymerization, blocking groups were removed. All molecules contained a single DNP label on the ϵ -amino group of the C-terminal lysine. Unlabeled, chromatographically purified oligolysines, (Lys)_m ($m = 3-8$), were part of a preparation described earlier (Yaron *et al.*, 1964).

ϵ -N-DNP-L-lysine was prepared from the copper salt of L-lysine. Its purity was verified by elemental analysis and by thin layer chromatography (Eastman chromatograms) in 70% 1-propanol-30% ammonia.

Polynucleotides. Poly A (lots 13633, 15634, and 110638), poly U (lots 45443 and 48646), poly I (lot 35619), poly C (lots 212520 and 27622), and poly G (lot 5171) were purchased from Miles Chemical Co., Elkhart, Ind.; poly I (lot 6701) was purchased from Schwarz BioResearch, Orangeburg, N. Y. Poly A

* From the Laboratory of Biochemistry, National Cancer Institute, National Institutes of Health, U. S. Public Health Service, Department of Health, Education, and Welfare, Bethesda, Maryland 20014. Received July 10, 1967. Reprint requests should be sent to this address.

† Present Address: The Biophysics Research Laboratory, Department of Biological Chemistry, Harvard Medical School, Boston, Mass. 02115.

¹ Abbreviations used: ϵ -DNP-Lys(Lys)_n, L-(Lys)_n- ϵ -N-DNP-L-lysine; poly (A + U) and poly (I + C) represent association between polyadenylic and polycytidylic acid chains and between polyinosinic and polycytidylic acid chains, respectively.

(Miles 110638), poly U (Miles 48646), poly I (Schwarz 6701), and poly C (Miles 27622) were used in all but the early sets of experiments in 0.15 M NaCl. All but a few of the earlier batches of polymers were dialyzed against 0.01 M EDTA (pH 6–7)–0.2 M NaCl and metal-free water and then lyophilized before use. All polynucleotides were stored at -20° in a vacuum desiccator.

Dialysis Tubing. Visking (0.39 in. wide \times 0.002 in. thick) tubing was used. It was cut into 4–5-ft strips, boiled in 0.2 M Na_2CO_3 –0.01 M EDTA for 30 min, then rinsed, and flushed with water.

Methods

Oligolysines. The ϵ -DNP-Lys(Lys) $_n$ mixture was fractionated on CM-cellulose essentially as described by Schlossman *et al.* (1965). Purified oligomers were examined in an amino acid analyzer and found to be better than 98% pure by ninhydrin analysis. Rechromatography of a mixture of the six purified oligomers used in this study ($n = 3$ –8) showed a regular progression of peaks, no peak omitted.

Chain-length assignments were obtained by measuring total ninhydrin (after acid hydrolysis), using a lysine-HCl standard and OD_{360} . The assignments were consistent with results of analytical chromatography on CM-cellulose of the original mixture.

The ϵ -DNP-oligolysines were stored frozen. Following dialysis experiments, the unbound compounds were reclaimed by desalting as described by Schlossman *et al.* (1965). Such reclaimed material was reexamined by analytical chromatography and shown to be unchanged, ruling out breakdown of the oligolysines during the dialysis experiments.

The molar extinction coefficient at 360 $m\mu$ (ϵ_{360}) for ϵ -N-DNP-L-lysine was found to be 17,450 in 0.05 M NaCl or 0.15 M NaCl, buffered by 0.01 M cacodylate (pH 7.0), in good agreement with data in the literature (Carsten and Eisen, 1953; Ramachandran and Sastry, 1962). The ϵ -N-DNP-L-lysine was photostable as reported previously by Russel (1963).

Measurement of $\text{OD}_{260}:\text{OD}_{360}$ was 0.477 ± 0.005 for ϵ -N-DNP-L-lysine as well as the ϵ -DNP-oligolysines. This is evidence for the complete removal from the ϵ -DNP-oligolysines of the aromatic blocking group used in the synthesis.

Concentrations of unsubstituted oligolysines were determined in terms of lysine following acid hydrolysis. Such analyses agreed with values calculated on the basis of dry weight to within a few per cent.

Polynucleotides. All polymer preparations were screened by chromatography on Sephadex G-100 in 0.25 M NaCl–0.001 M sodium phosphate (pH 7), conditions under which tRNA is only partially excluded. Only principally excluded polymer material was used in these experiments reported here.

Extinction coefficients, based on micromoles of phosphorus, were determined for all synthetic polynucleotides using the micromethod of Ames and Dubin (1960). Optical densities were determined at 22–24 $^{\circ}$ in

0.15 M NaCl–0.01 M sodium cacodylate (pH 7.0), and all polynucleotide solutions were made up and assayed in this buffer. The molar extinction coefficients of poly A at 257 $m\mu$ were (Miles 13633) 11.5×10^3 , (Miles 15634) 10.6×10^3 , and (Miles 110638) 10.4×10^3 ; poly U at 260 $m\mu$ (Miles 45643) 9.8×10^3 and (Miles 48643) 9.5×10^3 ; poly C at 268 $m\mu$ (Miles 212520) 6.65×10^3 and (Miles 27622) 6.68×10^3 ; poly I at 248 $m\mu$ (Miles 35619) 11.2×10^3 and (Schwarz 6701) 10.6×10^3 ; and poly G at 253 $m\mu$ (Miles 5171) 10.8×10^3 .

Mixing curves were obtained by the method of continuous variation using the extinction coefficients described above and were of the form expected (Steiner and Beers, 1961). Reaction of poly I plus poly C to form a 1:1 complex, poly (I + C), was monitored by optical density measurements at 235 $m\mu$. Reaction of poly A and poly U to form poly (A + U) at a 1:1 A:U mole ratio and poly (A + 2U) at a 1:2 A:U mole ratio was followed by optical density measurements at 260 and 280 $m\mu$ as described by Stevens and Felsenfeld (1964).

For poly G plus poly C, a discontinuity in the slope of the mixing curve was found at a 1:1 G:C molar ratio when measured at 245, 262, and 280 $m\mu$ as described by Pochon and Michelson (1965), with the effect at 262 $m\mu$ being one of *hyperchromism*. Because of this effect and the general lack of knowledge about poly (G + C) structure, this 1:1 complex might not be a typical two-stranded helix.

Hypochromism on complex formation for poly (I + C) at 235 $m\mu$ averaged 30%; that for poly (A + U) 28% at 260 $m\mu$ and 1% at 280 $m\mu$, and for poly (A + 2U) 35% at 260 $m\mu$ and 21% at 280 $m\mu$. For the 1:1 poly G–poly C complex, hypochromism was 12% at 245 $m\mu$ and 19% at 280 $m\mu$, with 10% hyperchromism at 262 $m\mu$.

Stock solutions at 3–5 mM phosphorus of two- and three-stranded polynucleotides were made up in 0.15 M NaCl–0.01 M sodium cacodylate (pH 7.00) using the above extinction coefficients and stored frozen. Aliquots for a given set of experiments were taken from the same stock solution (usually with the same pipet) reducing the error within a set of experiments as compared to that between sets.

Sedimentation coefficients were determined on all complexes in an ultracentrifuge using ultraviolet optics. Values of $s_{20,\text{buffer}}$ for poly (I + C) and poly (A + U) ranged from 9.2 to 13.5. No correlation between $s_{20,\text{buffer}}$ and oligolysine binding strength was observed. $s_{20,\text{buffer}}$ for poly (A + 2U) was 15.2. The poly G–poly C complex was a rapidly sedimenting aggregate.

Equilibrium Dialysis Experiments. In a standard dialysis experiment, 1 cc of polynucleotide solution was pipetted into a section of dialysis tubing, which was tied at both ends, weighed, and then placed into 10 ml of buffer (containing oligolysine) in a Nalgene tube. The tube was covered with parafilm and placed on a rotating turntable in a 4 $^{\circ}$ room. Equilibrium approach was monitored by withdrawing samples of the dialysate from duplicate tubes. Results were cal-

culated from samples taken after the monitor tube showed no detectable change for at least 1 day. This period of time was usually 5–7 days. It should be noted that this time is much greater than that expected from measurements of approach to equilibrium in the absence of polynucleotide.

Once equilibrium was reached, the optical densities at 360 $m\mu$ of the inside and outside solutions were measured in a Zeiss PMQ II spectrophotometer equipped with a slit adjustment and magnetic cell positioner, generally with 1-cm path-length cells, although 0.5-cm path-length cells were used for optical densities over 1.5 and 5-cm cells for optical densities under 0.1. Since hypochromism of the DNP at 360 $m\mu$ was detected on binding of the DNP-oligolysine to the polynucleotide, and since ΔH for the binding was not known, readings of the sack contents were done at $4 \pm 1^\circ$ maintained by circulating water from an ice bath through a Zieler heatable cell holder in the Zeiss spectrophotometer. There was little loss of OD_{360} material due, for example, to adsorption to the Nalgene tube or the dialysis tubing.

Readings at 260 $m\mu$ showed that an average of less than 1–2% of the polynucleotide passed out of the sack. Optical density blanks due to the tube and tubing were always very low. Sack contents were monitored in the range 260–290 $m\mu$ (depending on the polynucleotide concentration and cuvet path length). Short of precipitation, no significant change in absorbance due to the polynucleotide was seen, ruling out material loss due to aggregation or adsorption during binding, and (when done at 280 $m\mu$) ruling out $2 \text{ poly (A + U)} \rightleftharpoons \text{poly (A + 2U)} + \text{poly (A)}$ inter-conversion on oligolysine binding. Soluble aggregates, if present, did not spin down at 2000g for 15 min. At much lower concentrations, using ultraviolet optics in the ultracentrifuge, aggregation resulting from complex formation was not found. However, once visible precipitation occurred, OD_{260} measurements following the low-speed centrifugation showed loss of much and sometimes all of the polynucleotide from solution.

Changes in sack volume were monitored by weighing the sack (after wiping) immediately after preparation and immediately before reading. Volume changes of up to 15% were not uncommon. This method was calibrated by a series of experiments in which high molecular weight Blue Dextran was placed in the sack, and changes in OD_{620} and sack weight were compared. The results agreed closely with those expected assuming that all OD_{620} changes were due to a concentration increase of the Blue Dextran inside the sack resulting from such volume decrease.

Binding reversibility was checked by running a duplicate tube through the experiment, transferring the sack after equilibrium was reached into a fresh buffer solution free of oligolysine, and reequilibration. Results so obtained were very similar or identical with those of the binding curves unless precipitation of the polynucleotide-oligolysine complex had occurred.

Experiments of oligolysine binding to poly (I + C)

and poly (A + U) were done in paired tubes initially identical except for the polynucleotide. Higher final OD_{360} readings inside the sacks containing poly (I + C) as compared with those containing poly (A + U) were accompanied by lower solution OD_{360} readings outside the sacks, ruling against any optical artifact such as scattering as the cause of the difference in measured binding.

Melting curves were performed according to Felsenfeld and Sandeen (1962).

Results

A set of curves representing the binding of ϵ -DNP-oligolysines to poly (I + C) and poly (A + U) is shown in Figure 1. At 0.15 M NaCl, binding was easily measurable over the oligolysine size range shown. This concentration of salt is well above that needed to suppress any Gibbs-Donnon effect due to the polynucleotide, a point corroborated by lack of dependence of the binding on polynucleotide concentration.

A number of qualitative observations can be made from these binding curves. First of all, binding of a given oligomer to poly (I + C) generally exceeds that to poly (A + U). The difference between the initial slopes of the poly (I + C) and poly (A + U) binding curves increases with oligomer size. In addition the amount of the oligolysine-polynucleotide interaction greatly increases with increasing oligolysine chain length. *Since the binding varies much more with oligomer size than with polynucleotide species, the detection of binding specificity depends on the use in any particular experiment of purified oligolysines of a single chain length.*

The shapes of the poly (I + C) and poly (A + U) binding curves differ. Those for poly (I + C) resemble the theoretical isotherms for colinear oligomer-polymer binding calculated and diagrammed in the Appendix (see Figure 9, in the Appendix). Less curvature exists in the plots of oligolysine binding to poly (A + U). While this could be due to a cooperative feature of the binding process, such an effect is probably not large since inflection points are not seen in the binding curves and since melting curves at low saturation of polynucleotide by oligolysine (*e.g.*, 20%) indicate that, at least near the observed melting temperatures, the binding does not follow an all-or-none behavior. In addition to shape differences, the curves of the binding of longer oligolysines to poly (A + U) end in precipitation. The minimum oligomer size for this precipitation decreases with decreasing buffer ionic strength.

The curves for ϵ -DNP-Lys(Lys)₆ (Figure 1D) are particularly instructive in consideration of specificity. Measurements of binding as soluble complexes clearly indicate a preference of ϵ -DNP-Lys(Lys)₆ for poly (I + C) over poly (A + U) at the solvent conditions used. However, if precipitation is used as the criterion, one would conclude the converse, since only poly (A + U) complexes precipitate. Furthermore, concomitant with

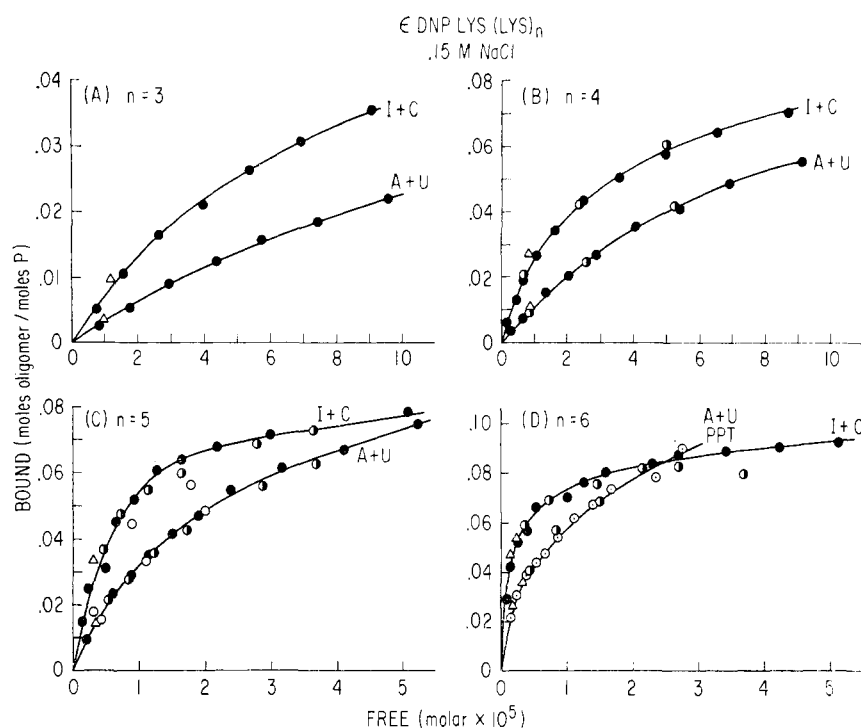


FIGURE 1: ϵ -DNP-Lys(Lys) $_n$ ($n = 3-6$) binding to poly (I + C) and poly (A + U) in 0.15 M NaCl buffered by 0.01 M sodium cacodylate-cacodylic acid (pH 7.0). Calculation of ordinate and abscissa explained in text. Points marked Δ are reversibility checks reequilibrated with buffer from higher degrees of saturation. Polynucleotide concentrations (in 1 mM P): (A) solid circles, 3.23; (B) solid circles, 2.16; half-circles, 1.08; (C) solid circles, 1.08; half-circles, 0.461; open circles, 1.94; and (D) solid and dotted circles, 0.808; half-circles, 0.404.

poly (A + U) precipitation there occurs a sharp increase in association of the oligolysine with the polynucleotide. This is demonstrated by measurement of the final concentration of free oligolysine for paired points of binding curves to poly (I + C) and poly (A + U) which started out with the same total amount of oligolysine and polynucleotide (Figure 2). Prior to precipitation of the poly (A + U), the free ϵ -DNP-oligolysine concentration is greater in the poly (A + U) tubes. However, once precipitation has occurred, more oligolysine binding occurs to poly (A + U). The sharp transition at precipitation can be seen in Figure 2. This type of "cooperative" phenomenon is probably secondary to an aggregation tendency of the poly (A + U)-oligolysine complex as the complex approaches charge neutralization. In the presence of the high charge density of the resulting coacervate (Overbeek and Voorn, 1957), an increased attraction could be created for the free oligolysine, the process snowballing until precipitation occurs. Thus cooperative effects can override and mask binding affinities and should be considered in any interpretation of experiments aimed at comparing specificities.

Binding of ϵ -DNP-oligolysine to poly (A + 2U) is shown in Figure 3. For poly (A + 2U), the low isotherm curvature and precipitation tendencies are even more pronounced than with poly (A + U) although short of precipitation complexes formed did not spin

out under the conditions used and binding reversibility was present. The magnitude of the binding to poly (A + 2U) is similar to that to poly (I + C) and poly (A + U), supporting the idea that specific sites on the polynucleotide are bound to the oligolysine. If binding were merely nonspecific immobilization of the oligolysine in the vicinity of the polynucleotide, binding to poly (A + 2U) with its much greater linear charge density would be expected to greatly exceed that to poly (A + U) or poly (I + C). Oligolysine binding to the aggregated poly G-poly C complex was strong and reversible, with no precipitate formation. Quantitation of this binding is uncertain because of the physical state of the polynucleotide and considerable scattering resulting from this state.

The effect of ϵ -DNP-oligolysine binding on DNP ϵ_{360} was measured by adding identical amounts of oligolysine to solutions of identical volumes with only one containing polynucleotide, under conditions where, according to the above curves, binding of the oligolysine is nearly complete. Assuming conservation of oligolysine in solution, the free oligomer concentration can be estimated from the isotherms and used as a small correction in determining binding hypochromism from the OD $_{360}$ differences measured. The results were independent of oligomer chain length for ϵ -DNP-Lys(Lys) $_n$, $n = 5, 6$, or 7, with the average value for the ratio ϵ_{360} bound: ϵ_{360} free = H being 0.77 for

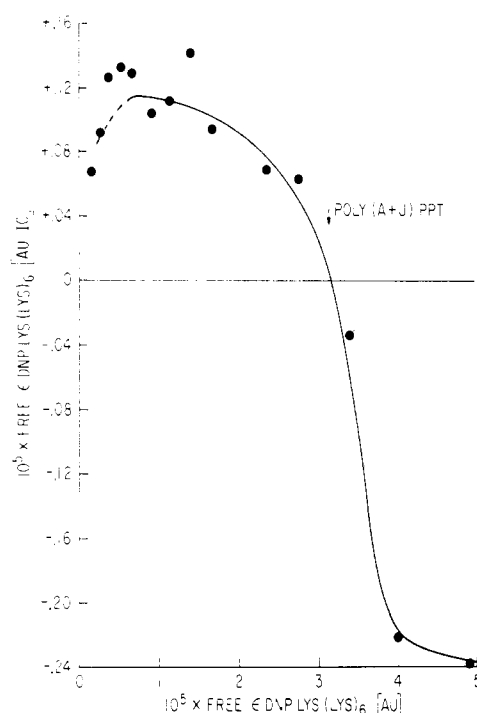


FIGURE 2: Effect of poly (A + U)- ϵ -DNP-oligolysine complex precipitation on additional ϵ -DNP-oligolysine binding. Experiments with poly (A + U) and poly (I + C) were done in paired tubes with the same total initial amount of ϵ -DNP-oligolysine in both members of a pair. A lower final free ϵ -DNP-oligolysine concentration then reflects higher binding to the polynucleotide. ϵ -DNP-oligolysine binding to poly (I + C) thus exceeds that to poly (A + U) until poly (A + U) precipitation occurs, when the reverse holds.

poly (I + C) and 0.73 for poly (A + U). In addition, small shifts in ϵ -DNP-absorption maxima were observed upon ϵ -DNP-oligolysine binding to the polynucleotides. The existence of these spectral changes underlines the need for considering the role of the DNP group in any effects obtained with ϵ -DNP-oligolysines.

Analysis of Curves

The theoretical basis for the analysis used is given in the Appendix. The basic formula (*cf.* eq 20 of Appendix) which describes the binding reasonably well (for $\alpha < 0.5$) is

$$\alpha = \frac{aK_0C}{1 + (a + \gamma)K_0C}$$

where α = fractional coverage of the polynucleotide by oligolysine; K_0 = intrinsic oligomer-polymer binding constant; C = free oligolysine concentration; a = effective number of polymer sites covered per oligolysine; and γ = a constant, the value of which depends on a .

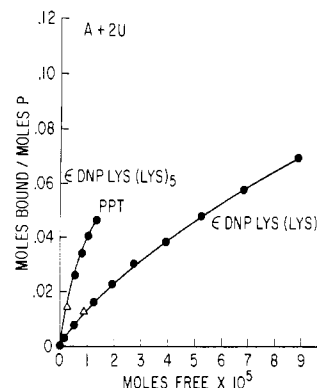


FIGURE 3: ϵ -DNP-oligolysine binding to poly (A + 2U) in 0.15 M NaCl-0.01 M sodium cacodylate-cacodylic acid (pH 7.0). Points marked Δ are reversibility checks. Poly (A + 2U) concentration was 2.12 mM P.

With the experimental quantities $B = OD_{360}$ bound/micromole of phosphorus and $F = OD_{360}$ free proportional to α/a and C , respectively, one can show that a plot of $1/B$ vs. $1/F$, a reciprocal plot, will give a slope $X = 10^3/HK_0$, and a plot of B/F vs. B , or Scatchard plot, will yield a $B = 0$ intercept I such that $K_0 = I/H \times 10^3$. The intercept of the reciprocal plot and the slope of the Scatchard Plot both underestimate the saturation by a factor $a/(a + \gamma)$, where $\gamma > 0$ for oligomer binding. However, the determination of K_0 is independent of estimates of a or γ .

Values of $\log K_0$ (K_0 in M^{-1}) given in Tables I and II were obtained from the average of Scatchard and reciprocal plots (which were in good agreement) of binding curves like those described earlier. Also calculated was the ratio R , where $R = K_{IC}/K_{AU}$ is a measure of the binding preference of an ϵ -DNP-oligolysine for poly (I + C) over poly (A + U). The energies of binding and specificity are proportional to $\log K_0$ and $\log R$, respectively.

Plots are shown of $\log K_{IC}$ (Figure 4) and $\log R$ (Figure 5) vs. oligolysine size. Because $\log R$ is so much smaller than $\log K_{IC}$, the curves for $\log K_{AU}$ would be very close to those for $\log K_{IC}$ at the scale used and thus a plot of $\log R$ is considered more descriptive.

The dependence of $\log K_{IC}$ on NaCl concentration and oligolysine size is apparent, as is the increase of $\log R$ with oligolysine size. The data scatter is too great to allow conclusions about any dependence of $\log R$ on NaCl concentration. The line drawn assumes the absence of any dependence of $\log R$ on NaCl concentration. The weighted least-squares increment in $\log R$ /residue is 0.06.

Confirmation beyond that resulting from the dependence of $\log R$ on oligomer size that the specificity seen was not an artifact due to the DNP group was obtained from competition experiments. Equal amounts of an unlabeled oligolysine were added to paired duplicate tubes in an experiment measuring DNP-

TABLE I: ϵ -DNP-Oligolysine-Polynucleotide Binding Constants.^a

ϵ -DNP-Lys(Lys) _n		0.15 M NaCl				
		Set 1	Set 2	Set 3	Set 4	Av
<i>n</i> = 3	Poly (I + C)	2.88	2.69	2.71	2.88	2.79
	Poly (A + U)	2.63	2.47	2.47	2.54	2.53
	Ratio <i>K</i> _{IC} : <i>K</i> _{AU}	0.25	0.22	0.24	0.34	0.26
<i>n</i> = 4	Poly (I + C)	3.45	3.34	3.28	3.55	3.41
	Poly (A + U)	3.16	3.03	3.06	3.10	3.09
	Ratio <i>K</i> _{IC} : <i>K</i> _{AU}	0.29	0.31	0.22	0.45	0.32
	Poly (A + 2U)				3.21	
<i>n</i> = 5	Poly (I + C)	4.10	3.89	3.89	4.22	4.02
	Poly (A + U)	3.66	3.56	3.54	3.74	3.62
	Ratio <i>K</i> _{IC} : <i>K</i> _{AU}	0.44	0.33	0.35	0.48	0.40
<i>n</i> = 6	Poly (I + C)	4.48	4.38	4.69	4.77	4.58
	Poly (A + U)	4.15	4.02	4.17	4.31	4.16
	Ratio <i>K</i> _{IC} : <i>K</i> _{AU}	0.33	0.36	0.52	0.46	0.42

^a Measurement and equilibration at 4°. For calculation of binding constants, see text. Binding constants expressed as log of values.

oligolysine binding to poly (I + C) and poly (A + U) under conditions where the two oligomers had the same magnitude of binding strengths. The binding of the unlabeled oligomers was then estimated as described in the Appendix from their competition with the DNP-oligolysine binding and the poly (I + C)/poly (A + U) preference of the unlabeled oligomer relative to that of the labeled oligomer determined. This last value can be obtained from the binding without the competitor and thus the specificity of the competitor is found. A binding curve demonstrating this effect is shown for the case of ϵ -DNP-Lys(Lys)₅ as indicator and (Lys)₈ as competitor (Figure 6). Results tabulated below (Table III) give oligomer specificity and indicator specificity. All oligomers showed a specificity toward poly (I + C) in the buffers used. Furthermore, the relative magnitudes of the unlabeled oligomer and DNP oligomer specificities increased with chain length.

Determination of the saturation of oligomer binding to polynucleotide from a binding curve is difficult unless some knowledge or assumption exists about *a*, the number of polymer sites covered per oligomer. Unlike binding curves for monomers, oligomer isotherms reach a very gradual plateau which only slowly exceeds 80% saturation, with little dependence on oligomer size above the tetramer or pentamer. This behavior makes extrapolation procedures from linear plots impossible.

Two approaches were used to estimate saturation, one for ϵ -DNP-oligolysine, the other for unlabeled oligolysine. The first compares the observed plateaus of binding curves for different ϵ -DNP-oligolysines with those expected at a saturation value (α) of 0.8 using a range of values of *a* and the standard

curves (see Figure 9 in the Appendix). Since *a* is the number of polymer sites covered per oligomer, the lysine:phosphate ratio at saturation is *n*:*a*. Figure 7 shows curves of ϵ -DNP-Lys(Lys)_n binding to poly (I + C) at salt concentrations chosen to allow for strong binding for all oligomers. The reduced curvature at high saturation and precipitation of the poly (A + U) makes a similar analysis impossible for poly (A + U). Plateaus (assuming $\alpha = 0.8$ at these levels) occur for values of *a* between *n* + 2 and *n* + 3. This relationship found between *a* and *n* supports the idea that the difference between them is due to end effects. Much of this difference is undoubtedly due to the single bulky ϵ -DNP-lysine terminal residue which contributes to *a* but not to *n*.

The second approach, independent of the first, utilizes the competition between an unlabeled oligomer and the ϵ -DNP-oligomer. Oligomer sizes are chosen so that under the experimental conditions the unlabeled oligomer (unlike the DNP oligomer) binds nearly completely. Then, knowing the amount of this oligomer added and calculating the fraction (α_m) of the polynucleotide saturated from the change caused in the binding of the ϵ -DNP oligomer and the original amount of ϵ -DNP oligomer binding, the equivalence ratio of the unlabeled oligolysine-polynucleotide complex *in solution* can be estimated. As a first approximation

$$\alpha_m = 1 - \frac{(\text{OD}_{360} \text{ bound}/\mu\text{mole of P})_1}{(\text{OD}_{360} \text{ bound}/\mu\text{mole of P})_2}$$

where 1 and 2 refer to DNP oligomers binding at the same free concentration with and without competition

TABLE II: ϵ -DNP-Oligolysine-Polynucleotide Binding Constants (log).

ϵ -DNP-Lys(Lys) _n		0.25 M NaCl			0.39 M NaCl	0.50 M NaCl	0.02 M NaCl
		Set 1	Set 2	Av			
$n = 3$	Poly (I + C)	2.20	2.23	2.21			4.92
	Poly (A + U)	1.94	1.89	1.91			4.72
	Ratio = $K_{IC}:K_{AU}$	0.26	0.34	0.30			0.20
							0.06 M NaCl
$n = 4$	Poly (I + C)	2.85	2.86	2.85	2.04		4.97
	Poly (A + U)	2.40	2.39	2.39	1.60		4.62
	Ratio = $K_{IC}:K_{AU}$	0.45	0.47	0.46	0.44		0.35
							0.10 M NaCl
$n = 5$	Poly (I + C)	3.23	3.21	3.22	2.23		5.07
	Poly (A + U)	2.80	2.79	2.79	1.88		4.71
	Ratio = $K_{IC}:K_{AU}$	0.43	0.42	0.43	0.35		0.36
$n = 6$	Poly (I + C)	3.77	3.63	3.70	2.56	1.84	
	Poly (A + U)	3.18	3.12	3.15	2.13		
	Ratio = $K_{IC}:K_{AU}$	0.59	0.51	0.55	0.43		
$n = 7$	Poly (I + C)	4.13	4.08	4.10	2.74	2.05	
	Poly (A + U)	3.57	3.54	3.55	2.26		
	Ratio = $K_{IC}:K_{AU}$	0.56	0.54	0.55	0.48		
$n = 8$	Poly (I + C)	4.40				2.24	
	Poly (A + U)	3.82				1.95	
	Ratio = $K_{IC}:K_{AU}$	0.58				0.29	

from (Lys)_m, the unlabeled oligomer. If the oligomer-polymer model discussed holds, a small correction (Δ) defined in the Appendix must be subtracted from α_m because of the effect of the competitor on the arrangements of the free and ϵ -DNP oligomer bound sites. The results are tabulated below (Table IV) as equivalents of phosphorus covered per equivalents of lysine bound with and without Δ for poly (I + C) and poly (A + U). The average values for poly (I + C) are 0.99 without Δ and 0.87 with Δ , and for poly (A + U) 0.85 without Δ and 0.73 with Δ . Most of the possible experimental errors are such as to increase this ratio by a few per cent. However, the amount of free oligomer was proved less than 1% of the total added by examining the final

dialysate fluid in an amino acid analyzer. Note that the difference between the observed values and 1.0 is in the opposite direction from the results of Tsuboi *et al.* (1966) and Higuchi and Tsuboi (1966). From indirect estimates based on melting studies, these authors found ratios of 2.0 for poly (I + C) and 1.5 for poly (A + U). The difference between poly (I + C) and poly (A + U) found in our work is much smaller than that found by these authors, and may in part be due to a cooperative component of the binding to poly (A + U). This would result in a smaller than otherwise expected drop in ϵ -DNP-oligolysine binding due to an increased affinity of the ϵ -DNP-oligolysine for the remaining sites of the poly (A + U) once the unlabeled oligolysine is bound.

TABLE III

ϵ -DNP-Lys(Lys) _n	(Lys) _m	ϵ -DNP-Lys(Lys) _n $K_{IC}:K_{AU}$	(Lys) _m $K_{IC}:K_{AU}$
ϵ -DNP-Lys(Lys) ₃ ^a	(Lys) ₃	1.6	1.5
ϵ -DNP-Lys(Lys) ₄ ^b	(Lys) ₄	2.2	1.7
ϵ -DNP-Lys(Lys) ₆ ^c	(Lys) ₆	2.7	3.5
ϵ -DNP-Lys(Lys) ₇ ^c	(Lys) ₈	3.6	5.3

^a 0.02 M NaCl. ^b 0.06 M NaCl. ^c 0.25 M NaCl.

Discussion

The linearity of the log K_{IC} plots as well as the strong dependence on NaCl concentration is apparent. The slopes (S) or $\Delta \log K_{IC}/\Delta n$ are 0.60 at 0.15 M NaCl, 0.47 at 0.25 M NaCl, 0.26 at 0.39 M NaCl, and 0.20 at 0.50 M NaCl. The results are consistent with the idea that all the ϵ -NH₃⁺ groups of an oligolysine have roughly equivalent interactions with the polynucleotide phosphates, implying some regularity in the structure of the complexes formed. The extrapolation to $n = 0$ may or may not be justified as representing the binding constant of ϵ -DNP-lysine, but the convergence

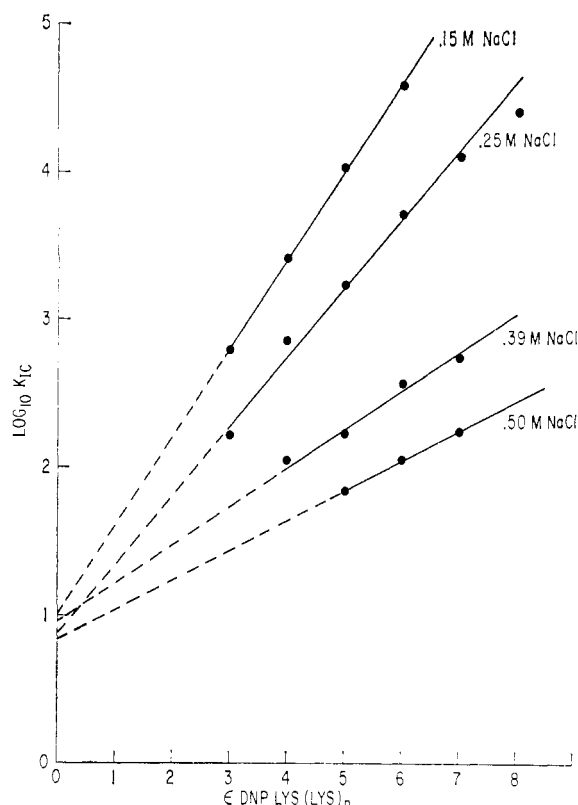


FIGURE 4: $\log K_{IC}$ for ϵ -DNP-Lys(Lys) $_n$ binding to poly (I + C) in 0.15 M NaCl, 0.25 M NaCl, 0.39 M NaCl, and 0.50 M NaCl, all at 0.01 M sodium cacodylate-cacodylic acid (pH 7.0). Calculation of K_{IC} explained in the text.

of the extrapolations for the different NaCl concentrations supports the idea that the NaCl affects only the binding of the charged ϵ -NH $_3^+$ groups.

As shown in the Appendix, a model in which the Na $^+$ competes with the oligolysine for single sites on the polynucleotide predicts (Appendix eq 17 and 18) that

$$S = \frac{\Delta \log K_0}{\Delta n} \text{ should vary as } \log \left(\frac{K_0'}{1 + (qNa^+)Na^+} \right)$$

where K_0' is the intrinsic association constant increment per lysine residue and qNa^+ is the effective association constant of the Na $^+$, concentrations being used instead of activities. This could explain the extremely large effect on K_{IC} of only a relatively small change (0.15–0.50 M) in NaCl concentration and would predict that a plot of 10^{-S} vs. NaCl concentration would be linear. Such a plot is given in Figure 8. The straight line has an intercept of 0.075 and a slope of 1.14. From this, one can calculate that $K_{IC}' = 13 \text{ M}^{-1}$ and $qNa_{IC}^+ = 15 \text{ M}^{-1}$. The ratio of $qNa_{IC}^+ : K_{IC}'$ is probably more accurate than the absolute values. However, the value of 15 obtained predicts that at 0.2 M Na $^+$ (without oligolysines) a fraction equal to 0.75 of the

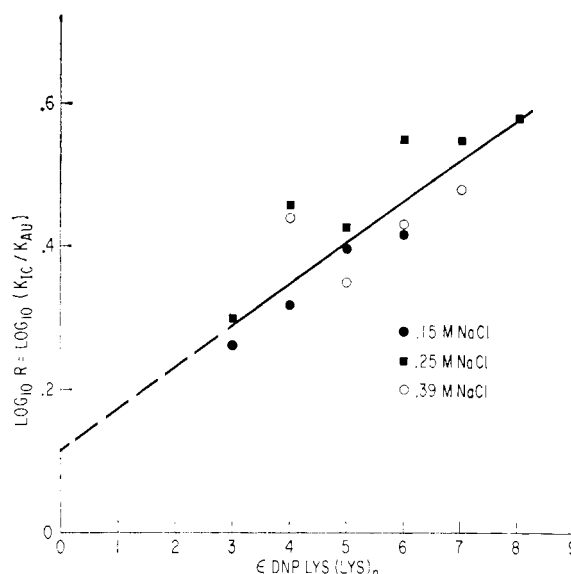


FIGURE 5: Binding specificity of ϵ -DNP-oligolysines. $\log R = \log K_{IC}/K_{AU}$ for ϵ -DNP-Lys(Lys) $_n$ binding to poly (I + C) and poly (A + U) in 0.15 M NaCl, 0.25 M NaCl, and 0.39 M NaCl, all at 0.01 M sodium cacodylate-cacodylic acid (pH 7.0).

phosphates will be covered by Na $^+$, a figure in excellent agreement with the value of 0.78 for DNA obtained by Strauss and Ross (1959).

The importance of the Na $^+$ binding to the polynucleotide is striking and must be considered in any interpretation of binding strength or specificity. The oligolysine competes favorably with the Na $^+$ only because binding of one residue results in binding of most or

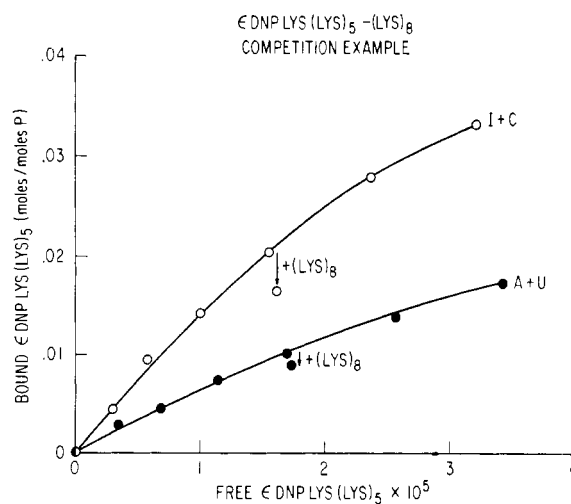


FIGURE 6: ϵ -DNP-Lys(Lys) $_5$ binding to poly (I + C) and poly (A + U) with effect of addition of 0.64 μ mole (as lysine) of Lys $_8$ in 0.25 M NaCl–0.01 M sodium cacodylate-cacodylic acid (pH 7.0). Polynucleotide concentration was 1.50 mM P.

TABLE IV: Oligolysine-Polynucleotide Saturation Ratio.^a

ϵ -DNP-Lys(Lys) _n Indicator	(Lys) _m	With Poly (I + C)	With Poly (A + U)
<i>n</i> = 3	<i>m</i> = 6	1.18 (1.08)	0.89 (0.80)
<i>n</i> = 3	<i>m</i> = 6	1.07 (0.88)	0.84 (0.66)
<i>n</i> = 3	<i>m</i> = 6	0.98 (0.80)	0.84 (0.67)
<i>n</i> = 4	<i>m</i> = 6	0.91 (0.84)	0.84 (0.80)
		Av 1.03 (0.90)	0.85 (0.73)
<i>n</i> = 3	<i>m</i> = 8	0.93 (0.79)	0.78 (0.63)
<i>n</i> = 3	<i>m</i> = 8	0.94 (0.80)	0.84 (0.69)
<i>n</i> = 5	<i>m</i> = 8	0.97 (0.87)	0.86 (0.75)
<i>n</i> = 5	<i>m</i> = 8	0.94 (0.85)	0.90 (0.81)
		Av 0.95 (0.83)	0.85 (0.72)
		Over-all av 0.99 (0.87)	0.85 (0.73)

^a Saturation ratio defined as nucleotide P:lysine. Number in parentheses includes estimate of correction for arrangement statistics.

all of the other residues even though a single lysine binds less strongly than Na⁺. The linearity of the plot in Figure 8 as well as the existence of strong oligolysine binding to poly (I + C) in 1 M tetramethylammonium chloride (to be described in more detail in the next paper) supports the assumption that the Cl⁻-oligolysine interaction is small.

The value of $\Delta F^\circ = -RT \ln K_{IC}'$ for the lysine-poly (I + C) interaction is -1.5 kcal. This is the molar binding energy per residue in the absence of competition from Na⁺. Even at 0.15 M NaCl, the effective ΔF° is reduced to -0.77 kcal. Thus binding constants obtained in buffers containing a significant amount of salt underestimate the true values.

With the binding following the above dependence on Na⁺ concentration, the convergence (Figure 4) at *n* = 0 of the extrapolated log *K*_{IC} curves has the more explicit interpretation that competition for the polynucleotide by Na⁺ with ϵ -DNP-Lys(Lys)_n occurs only for *n* sites per oligomer, further supporting the idea of a 1:1 ϵ -NH₃⁺-phosphate complex in solution. The nonzero intercept at *n* = 0 means only that some factor contributing to binding strength has a constant effect by *n* = 3 (the lowest point measured).

The dependence of log *R* (*R* = *K*_{IC}/*K*_{AV}) on *n* (Figure 5) is approximately linear but the data scatter prevents any conclusion about the variation of *R* with NaCl concentration. However, lack of a marked decrease in *R* with increased NaCl suggests that *R* is not solely due to a difference in charge density between poly (I + C) and poly (A + U). The weighted least-squares slope of the data is 0.06 or about 0.08 kcal/residue, a value tiny compared with $\Delta \log K_{IC}/\Delta n$ but still great enough when multiplied by polymer size to result in marked specificity. While the specificity might in fact be due to a difference in hydrophobic interactions between the oligomer and the two poly-

mers, it must be remembered that all measurements are made under conditions of strong competition between Na⁺ and the oligolysines, *i.e.*, one is in effect measuring the relative competition between the two cations for the anion. Cation effects on the binding will be investigated further in a later study.

The small but consistent differences in the binding of the oligolysines to poly (I + C) and poly (A + U), such as binding constant, isotherm shape, precipitability, and apparent saturation, all suggest some qualitative difference in the binding mechanism. The curve shape difference could be due to a cooperative effect on binding to poly (A + U). Since the binding to poly (I + C) exceeds that to poly (A + U) such a cooperative effect could not account for the specificity observed but if anything would decrease it.

While the different oligolysine binding properties of poly (I + C) and poly (A + U) may be merely functions of polynucleotide base composition, they might also be secondary to different sugar-phosphate backbone structures. For example, a difference in the polynucleotide structure *in solution*, such as translation along the helix axis per base pair, a parameter obtained from X-ray diffraction from fibers of 3.4 Å for poly (A + U) and 3.0 Å for poly (I + C) (Tomita and Rich, 1964) might be involved. Solution studies of polynucleotide-diamine interaction have been inferred as consistent with this (Gabbay, 1966).

However, the regular dependence of the binding strength on oligomer chain length and the estimated charge saturations are consistent with a model of colinear oligolysine-polynucleotide complex of regular structure for both poly (I + C) and poly (A + U), with ϵ -NH₃⁺ groups and phosphates in a 1:1 correspondence. Such an interaction is most easily constructed by having the oligolysine assuming an extended form and binding in one of the helical grooves, a

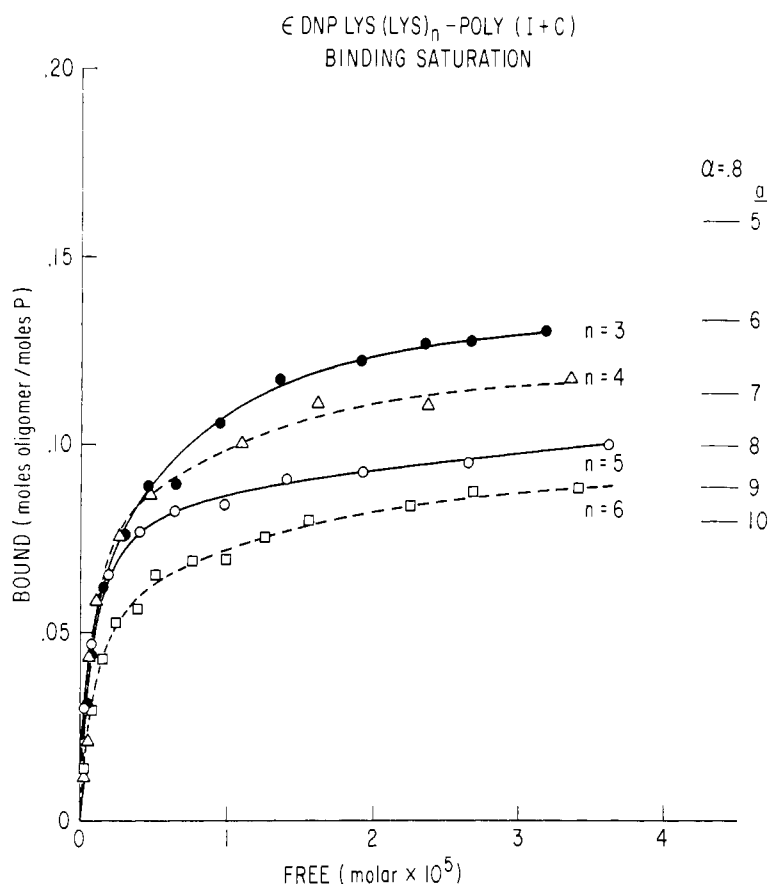


FIGURE 7: Binding of ϵ -DNP-Lys(Lys) $_n$ to poly(I + C) at NaCl concentrations reduced to allow for plateau ϵ -DNP-oligolysine binding. Solutions buffered at pH 7.0 as before. Lines at right-hand side drawn at level of binding that would be 0.8 of maximal saturation for values of a shown. a is defined in the Appendix as the number of polynucleotide sites covered by an oligolysine. Polynucleotide concentration and NaCl concentration: $n = 3$, 0.95 mM P, 0.02 M NaCl; $n = 4$, 0.86 mM P, 0.06 M NaCl; $n = 5$, 0.92 mM P, 0.10 M NaCl; and $n = 6$, 0.81 mM P, 0.15 M NaCl.

model suggested previously by Tsuboi *et al.* (1966) and Sober *et al.* (1966).

Appendix

The equations derived in this Appendix are used to interpret the results of studies measuring the binding of a series of oligolysines, ϵ -DNP-Lys(Lys) $_n$ ($n = 3-8$), to synthetic helical polyribonucleotides. The model used is that of adsorption at equilibrium of a linear oligomer of defined chain length to a linear polymer of much larger chain length. The treatment is extended to the case of a small number of different species of oligomers competing for the same polymer.

Binding equations will be obtained by two methods. The first is a combinatorial method which utilizes an expression for the number of arrangements of a given number of oligolysines bound to a polynucleotide. This method leads to equations involving nonreducible summations, making difficult the estimation of binding parameters from binding data. However, numerical evaluation of these equations yields theoretical binding curves which facilitate a qualitative interpretation of the

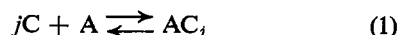
influence of oligomer size on binding curve shape. The second method uses the sequence generating function treatment of Lifson (1964), from which binding constants and stoichiometry can be obtained by data analysis.

Combinatorial Method

An oligocation of n singly charged residues is considered to bind colinearly to a much longer polyanion of N single sites in such a way as to make a adjacent sites on the polyanion unavailable to other oligocations ($a \geq n$). It will be assumed that the nature of the sites on the polyanion does not change during the binding and that the oligocations bind independently of one another. This last assumption implies that distant effects due to polyanion sites other than those being bound by a given oligocation are negligible compared with the local site binding forces. Such distant effects for a rigid polynucleotide at moderate ionic strengths (*e.g.*, 0.15 or higher) have been estimated to be relatively small (Schildkraut and Lifson, 1965).

Let A stand for the polyanion and C stand for the oligocation. Let ΔF_0 be the change in free energy for

the binding to a polyanion-oligocation complex of one additional oligocation to a *specified* sequence of a adjacent polyanion sites. $K_0 = e^{-\Delta F_0/RT}$ is the intrinsic oligomer-polymer binding constant. Then, for the binding of j oligocations to *any* available sets of a adjacent sites on the polyanion, a reaction expressed as



where AC_j represents the polyanion- j oligocation complex, the free-energy change can be expressed as $j\Delta F_0 + \Delta F_a$. The new term (ΔF_a) accounts for the different possible arrangements of the j -bound oligocations on the polyanion and is thus purely entropic, *i.e.*

$$\Delta F_a = -\Delta S_a T = -RT \ln \left(\frac{\Omega_j}{\Omega_0} \right) \quad (2)$$

where ΔS_a = the entropy change due to possible arrangements, Ω_j = the number of arrangements with j oligocations bound, and $\Omega_0 = 1$.

Designating the equilibrium constant for eq 1 as K_j , and using the symbols A , C , and AC_j to represent the activities of A , C , and AC_j

$$K_j = \frac{AC_j}{(A)(C)^j} = K_0^j \Omega_j \quad (3)$$

Ω_j is given by the number of ways of arranging j sets of a adjacent *covered* polymer sites and $(N - aj)$ *free* polymer sites, both possibilities counting as *one* statistical unit. Thus

$$\Omega_j = \frac{(N - aj + j)!}{(j)!(N - aj)!} \quad (4)$$

A more general discussion of this type of analysis is given by Silberberg (1962).

Finally, if V = the average number of molecules of oligomer bound per molecule of polymer, noting that $V_{\max} = N/a$

$$V = \frac{\sum_{j=1}^{j=N/a} j(AC_j)}{A + \sum_{j=1}^{j=N/a} AC_j} = \frac{\sum_{j=1}^{j=N/a} j \left[\frac{(N - aj + j)!}{(j)!(N - aj)!} \right] [K_0 C]^j}{1 + \sum_{j=1}^{j=N/a} \left[\frac{(N - aj + j)!}{(j)!(N - aj)!} \right] [K_0 C]^j} \quad (5)$$

When $a = 1$, eq 5 reduces (Tanford, 1961) to

$$V = \frac{NK_0 C}{1 + K_0 C} \quad (6)$$

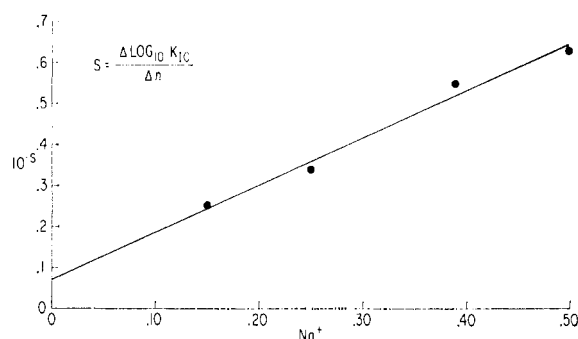


FIGURE 8: Effect of Na^+ concentration on $S = \log K_{1C}/\Delta n$. Slopes (S) obtained from Figure 4.

However, numerical evaluation of eq 5 is necessary for $a \geq 2$ since then the sums cannot be simply reduced.

Binding curves have been calculated for values of $a = 1-10$ and polyanion size $N = 50a$ using a CEIR computer. In Figure 9, dimensionless parameters are used, $\alpha = V/V_{\max}$ = fractional polynucleotide saturation being plotted against $K_0 C$. The values for α were shown to be nearly independent of polymer size N when $N \geq 25a$, the case $a = 6$ being evaluated in some detail for various N . This makes the above treatment applicable for large polyanions of polydisperse size such as polynucleotides of molecular weight in the range of 100,000 or more.

Compared with the isotherm for $a = 1$, isotherms for $a \geq 2$ become progressively more curved as a increases. Binding for $a \geq 2$ exceeds that for $a = 1$ in the early part of the curve but then is actually less than that for $a = 1$ with values of $\alpha = 0.8$ approached only very slowly. The bias against complete saturation of the polynucleotide at larger oligomer size and thus higher a is due to the sharp reduction in the number of arrangements of bound oligomers as the last few available blocks of a adjacent sites are covered.

Calculation of an "effective binding constant"

$$K_{\text{eff}} = \frac{(A_t - A)}{(A)(C)} \quad (7)$$

where A_t is the total polymer concentration assumes an isotherm like that for $a = 1$. If this treatment is applied to data for $a \geq 2$, the values of K_{eff} so obtained will exceed the true value (K_0) at low saturation but then be less than K_0 at high saturation. In fact, for a given K_0 , a wide range of values for K_{eff} can be obtained, the result depending on the saturation (α) at which K_{eff} is calculated.

Sequence Generating Function Method

Lifson considered the case of a polymer (of N sites) sufficiently large for end effects to be negligible. Then the partition function for this polymer, Z_N , can be written as x_1^N , where x_1 represents the contribution of each site to Z_N . For the case of two possible condi-

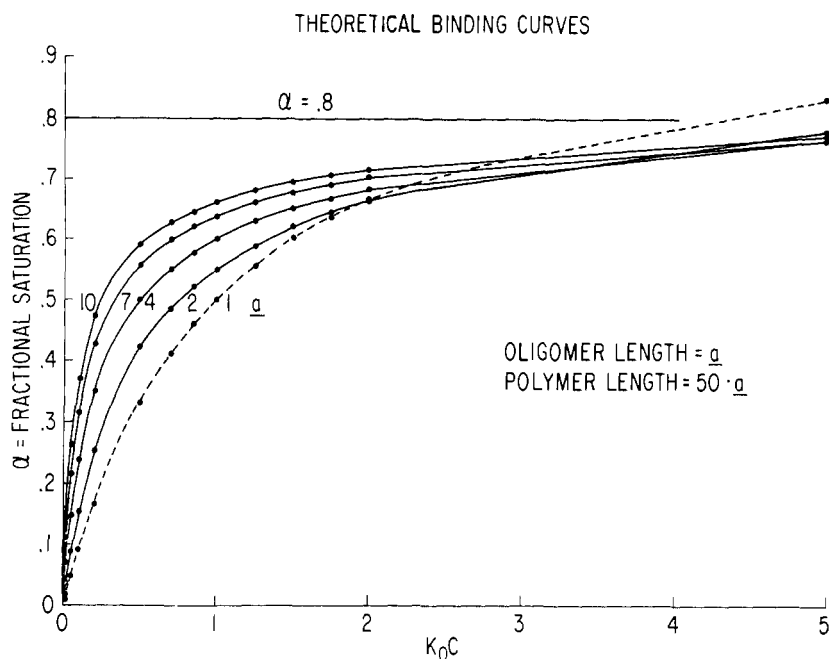


FIGURE 9: Theoretical curves calculated for colinear oligomer-polymer binding for values of a and polymer size = $50a$ (Appendix eq 5).

tions for a site on the polymer (unoccupied and occupied), $U = \sum_{j=1}^{\infty} u_j x^{-j}$ and $V' = \sum_{j=1}^{\infty} v_j x^{-j}$, where u_j is the statistical weight of j adjacent unoccupied sites, v_j is the statistical weight of j adjacent occupied sites, and x_1 is the largest root of $UV' = 1$. From $Z_N = x_1^N$, the thermodynamic functions of interest may be obtained.

Bradley and Lifson (1967) have presented a treatment applicable to the case of an oligomer at activity λ_a binding to a polymer and covering a adjacent sites. Making the same assumptions stated in our discussion of the combinatorial method, their expressions reduce to

$$U = \frac{q_0 x^{-1}}{1 - q_0 x^{-1}} \quad (8)$$

where q_0 = the statistical weight of an occupied site and

$$V = \frac{\lambda_a q_a x^{-a}}{1 - \lambda_a q_a x^{-a}} \quad (9)$$

where q_a = the statistical weight of a adjacent occupied sites. x_1 then becomes the largest root of

$$q_0 x^{-1} + \lambda_a q_a x^{-a} = 1 \quad (10)$$

Note that $q_a/(q_0)^a = q_a'$ and λ_a used here correspond to K_0 and C of the combinatorial method.

The average number of oligomers bound per single polymer (V) is given (e.g., Hill, 1960) by

$$V = \frac{\partial \ln Z_N}{\partial \ln \lambda_a} = N \frac{\partial \ln x_1}{\partial \ln \lambda_a} \quad (11)$$

and fractional coverage $\alpha = V/V_{\max}$ by

$$\alpha = a \frac{\partial \ln x_1}{\partial \ln \lambda_a} = \frac{a \lambda_a q_a x_1^{-a}}{q_0 x_1^{-1} + a \lambda_a q_a x_1^{-a}} \quad (12)$$

One feature of Lifson's method is that it can easily be extended to the case of two species of oligocations (e.g., occupying a and m sites, respectively) competing for binding to the polymer. The statistical weight of m adjacent polymer sites covered by the second oligocation species is denoted by q_m . Then the appropriate equations are

$$q_0 x^{-1} + \lambda_a q_a x^{-a} + \lambda_m q_m x^{-m} = 1 \quad (13)$$

$$\alpha_a = \frac{a \lambda_a q_a x_1^{-a}}{q_0 x_1^{-1} + a \lambda_a q_a x_1^{-a} + m \lambda_m q_m x_1^{-m}} \quad (14)$$

$$\alpha_m = \frac{m \lambda_m q_m x_1^{-m}}{q_0 x_1^{-1} + a \lambda_a q_a x_1^{-a} + m \lambda_m q_m x_1^{-m}} \quad (15)$$

For a univalent cation competing for single sites on the polymer (i.e., $m = 1$), eq 13 simplifies to eq 10 with the coefficient of x_1^{-1} now $q_0 + \lambda_1 q_1$ instead of

q_0 . Setting $q_1/q_0 = q_1'$

$$K_0 = \frac{q_a'}{(1 + \lambda_1 q_1')^a} \quad (16)$$

At any given λ_1 , $(1 + q_1'\lambda_1)^a$ simply enters into the expression for K_0 as a constant factor and thus would not affect the shape of the curves calculated using eq 5, justifying the neglect of this cation effect in the combinatorial method. One can express K_0 as

$$K_0 = \left(\frac{K_0'}{1 + \lambda_1 q_1'} \right)^a \quad (17)$$

where K_0' is the binding constant increment per occupied site.

Comparison of the Two Methods

The equivalence of the results of the combinatorial and sequence generating function methods can be checked for the case $a = 2$ since eq 10 then becomes a quadratic equation which can be solved exactly, *i.e.*

$$\frac{x_1}{q_0} = \frac{1 + \sqrt{1 + 4\lambda_a q_a'}}{2} \quad (18)$$

and

$$\alpha = \frac{\lambda_a q_a'}{\lambda_a q_a' + \frac{1}{4} + \frac{1}{4} \sqrt{1 + 4\lambda_a q_a'}} \quad (19)$$

Equation 19 predicts that the calculated curve for $a = 2$ (using eq 5) should intersect the curve for $a = 1$ at $1/4 + 1/4 \sqrt{1 + 4\lambda_a q_a'} = 1$ or $q_a'\lambda_a = K_0 C = 2$. This indeed occurs as can be seen in Figure 9. Also, $\alpha = V/V_{\max}$, calculated from eq 5 for various values of $K_0 C$ and N , approach those calculated from eq 19 (for $q_a'\lambda_a = K_0 C$) as N becomes large. For example, at $q_a'\lambda_a = 1$, eq 19 gives $\alpha = 0.550$ while the values of V/V_{\max} from eq 5 at $K_0 C = 1$ also approach 0.550.

Evaluation of K_0 from Binding Data

Equation 12 can be rewritten

$$\alpha = \frac{aK_0 C}{aK_0 C + \left(\frac{x_1}{q_0} \right)^{a-1}}$$

Empirically, by plotting $(x_1/q_0)^{a-1}$ vs. $K_0 C$, using eq 10, it was found that, for small $K_0 C$ (*e.g.*, $K_0 C \leq 0.5$), $(x_1/q_0)^{a-1}$ could be approximated by $1 + \gamma K_0 C$, where γ is a constant, the value of which depends on a . Then, setting $\alpha = aK_0 C / (1 + (a + \gamma)K_0 C)$

$$\frac{a}{\alpha} = \frac{1}{K_0 C} + (a + \gamma) \quad (20)$$

(The number of moles of oligomer bound per mole of polymer site, α/a , is experimentally measurable for singly labeled oligomers). The slope of a plot of a/α vs. $1/C$ can be used to obtain K_0 even without knowledge of a . However, the intercept of such a plot would give the incorrect value for α_{\max} of $a/(a + \gamma)$. Similar information can be obtained from the Scatchard plot (1949), α/C vs. α , since

$$\frac{\alpha}{C} = aK_0 - (a + \gamma)K_0\alpha \quad (21)$$

Evaluation of Binding Stoichiometry

Binding stoichiometry or the number of polymer sites complexed per oligomer residue can be estimated from an analysis of the effect of an unlabeled oligomer covering m polymer sites competing with the binding of a labeled oligomer covering a sites.

In the absence of competitor, the binding of the labeled oligomer can be written (from eq 12) as

$$(\alpha_a)_0 = \frac{a\lambda_a q_a x_{10}^{-a}}{q_0' x_{10}^{-1} + a\lambda_a q_a x_{10}^{-a}} \quad (22)$$

where $q_0' = q_0(1 + \lambda_1 q_1')$. With the competing oligomeric species added, setting $q_a'' = q_a/q_0'$ and $q_m'' = q_m/q_0'$

$$\alpha_a = \frac{a\lambda_a q_a'' x_1^{-a}}{x_1^{-1} + a\lambda_a q_a'' x_1^{-a} + m\lambda_m q_m'' x_1^{-m}} \quad (23)$$

and

$$\alpha_m = 1 - \frac{\alpha_a}{(\alpha_a)_0} - \Delta \quad (24)$$

where

$$\frac{\Delta}{\alpha_m} \approx \frac{\left[\frac{a-1}{m} \right] [1 - \alpha_m - \alpha_a]}{1 + \left[\frac{a-1}{m} \right] \alpha_m} \quad (25)$$

With the conditions such that only the (larger) unlabeled oligomer is completely bound, α_m can be compared with the amount of this competitor added. For example, if W equivalents of competing oligomer cover a fraction α_m of Y equivalents of polymer sites, then the complex between oligomer and polymer occurs at the ratio $W:\alpha_m Y$ on an equivalent basis. Such a determination can be obtained from measurements made *short* of polymer saturation and, except for the small correction term (Δ), depends only on the ratio $\alpha_a:(\alpha_a)_0$ obtained from a binding curve $((\alpha_a)_0$ vs. λ_a) and measurements of α_a made with competing oligomer added.

Competition Analysis of Relative Oligomer Binding to Two Polymer Species

One can use competition measurements to compare the relative binding strength of an unlabeled oligomer to two different species of polymer. In this case, one chooses conditions under which neither the indicator (occupying a polymer sites) nor the competitor (occupying m polymer sites) is completely bound. One then measures the relative preference of the competitor for one of the two polynucleotides compared with that of the indicator. Since the preference of the indicator can be obtained from separate experiments, one can calculate the ratio of the binding constant of the competitor to one polymer compared with that to the other polymer. From eq 24 α_m is still given by $1 - (\alpha_a/(\alpha_a)_0) - \Delta$, but when comparing α_m in two situations, Δ can be neglected and

$$\frac{(\alpha_m)_1}{(\alpha_m)_2} \approx \frac{\left(1 - \frac{\alpha_a}{(\alpha_a)_0}\right)_1}{\left(1 - \frac{\alpha_a}{(\alpha_a)_0}\right)_2} \quad (26)$$

with 1 and 2 referring to binding to polymers 1 and 2, respectively. One then has for the relative affinity of the competitor for the two polymers

$$\frac{q_{m1}''}{q_{m2}''} = \frac{(\alpha_{a2})_0 \lambda_{m2} \lambda_{a1} q_{a1}'' \left[\frac{\alpha_{m1}}{1 - \alpha_{m1}} \right] \left(\frac{x_1}{x_2} \right)^{-a+m}}{(\alpha_{a1})_0 \lambda_{m1} \lambda_{a2} q_{a2}'' \left[\frac{\alpha_{m2}}{1 - \alpha_{m2}} \right] \left(\frac{x_2}{x_1} \right)^{-a+m}} \quad (27)$$

measuring α_{m1} at λ_{m1} , λ_{a1} ; α_{a1} at λ_{m1} , λ_{a1} ; $(\alpha_{a1})_0$ at $\lambda_{m1} = 0$, λ_{a1} ; and similarly for polymer 2. If $m = a$, $(x_1/x_2)^{-a+m} = 1$. Otherwise, one can approximate $(x_1/x_2)^{-a+m}$ as

$$\left(\frac{x_1}{x_2} \right)^{-a+m} \approx 1 - (a - m) \left[\frac{\alpha_m}{m} \left(\frac{\Delta q_m''}{q_m''} + \frac{\Delta \lambda_m}{\lambda_m} \right) + \frac{\alpha_a}{a} \left(\frac{\Delta q_a''}{q_a''} + \frac{\Delta \lambda_a}{\lambda_a} \right) \right] \quad (28)$$

where $\Delta q_m'' = (q_m'')_1 - (q_m'')_2$ and $q_m'' = 1/2 \cdot ((q_m'')_1 + (q_m'')_2)$ etc., with the bracketed expression on the right-hand side of eq 28 being much less than 1.

Acknowledgments

The authors wish to express their thanks to Mr. Clyde Otey and Mr. James Williams for their assistance and proficiency in oligomer analysis; Mr. William White (Division of Computer Research and Technology, National Institutes of Health) for instruction in the

use of the CEIR computer; and Dr. Dan F. Bradley (National Institute of Mental Health, National Institutes of Health) for instructive discussions on the theoretical aspects of the Appendix. Particular appreciation is due Mrs. A. E. Stotler and Mrs. J. Shores for their patience and help in the preparation of this manuscript.

References

- Ames, B. N., and Dubin, D. T. (1960), *J. Biol. Chem.* 235, 769.
- Bradley, D. F., and Lifson, S. (1967), in *Molecular Associations in Biology*, Pullman, B., Ed., New York, N. Y., Academic.
- Carsten, M. E., and Eisen, H. N. (1953), *J. Am. Chem. Soc.* 75, 4451.
- Felsenfeld, G., and Sandeen, G. (1962), *J. Mol. Biol.* 5, 587.
- Gabbay, E. J. (1966), *Biochemistry* 5, 3036.
- Higuchi, S., and Tsuboi, M. (1966), *Biopolymers* 5, 837.
- Hill, T. (1960), *Introduction to Statistical Thermodynamics*, Reading, Mass., Addison Wesley.
- Lifson, S. (1964), *J. Chem. Phys.* 40, 3705.
- Nevo, A., De Vries, A., and Katchalsky, A. (1955), *Biochim. Biophys. Acta* 17, 536.
- Overbeek, J., and Voorn, M. (1957), *J. Cellular Comp. Physiol.* 49, Suppl. 1, 7.
- Pochon, F., and Michelson, A. M. (1965), *Proc. Natl. Acad. Sci. U. S.* 53, 1425.
- Ramachandran, L. K., and Sastry, L. V. S. (1962), *Biochemistry* 1, 75.
- Russel, D. W. (1963), *Biochem. J.* 87, 1.
- Scatchard, G. (1949), *Ann. N. Y. Acad. Sci.* 51, 660.
- Schildkraut, C., and Lifson, S. (1965), *Biopolymers* 3, 195.
- Schlossman, S., Yaron, A., Ben-Efraim, S., and Sober, H. A. (1965), *Biochemistry* 4, 1638.
- Silberberg, A. (1962), *J. Phys. Chem.* 66, 1884.
- Sober, H. A., Schlossman, S., Yaron, A., Latt, S. A., and Rushizky, G. W. (1966), *Biochemistry* 5, 3608.
- Steiner, R. F., and Beers, R. F., Jr. (1961), *Polynucleotides*, Amsterdam, Elsevier.
- Stevens, C., and Felsenfeld, G. (1964), *Biopolymers* 2, 293.
- Strauss, U., and Ross, P. (1959), *J. Am. Chem. Soc.* 81, 5295.
- Tanford, C. (1961), *Physical Chemistry of Macromolecules*, New York, N. Y., Wiley.
- Tomita, K., and Rich, A. (1964), *Nature* 201, 1160.
- Tsuboi, M., Matsuo, K., and T'so, P. O. P. (1966), *J. Mol. Biol.* 15, 256.
- Yaron, A., Berger, A., Katchalski, E., Otey, M. C., and Sober, H. A. (1964), *Abstr. 6th Intern. Congr. Biochem., New York*, 190.